CHMP1A encodes an essential regulator of BMI1-INK4A in cerebellar development

Ganeshwaran H. Mochida[1,2,3,4,5,*], **Vijay S. Ganesh**[1,2,3,6,*], **Maria I. de Michelena**[7], **Hugo Dias**[8], **Kutay D. Atabay**[1,2,3], **Katie L. Kathrein**[3,9,10,11], **Emily Huang**[3,9,10,11], **R. Sean Hill**[1,2,3], **Jillian M. Felie**[1,2,3], **Daniel Rakiec**[1,2,3], **Danielle Gleason**[1,2,3], **Anthony D. Hill**[12], **Athar N. Malik**[6], **Brenda J. Barry**[1,2,3], **Jennifer N. Partlow**[1,2,3], **Wen-Hann Tan**[1,4], **Laurie J. Glader**[4,13], **A. James Barkovich**[14], **William B. Dobyns**[15], **Leonard I. Zon**[3,4,9,10,11], and **Christopher A. Walsh**[1,2,3,4,16]

[1]Division of Genetics, Department of Medicine, Boston Children's Hospital, Boston, MA, USA

[2]Manton Center for Orphan Disease Research, Boston Children's Hospital, Boston, MA, USA

[3]Howard Hughes Medical Institute, Boston Children's Hospital, Boston, MA, USA

[4]Departments of Pediatrics, Harvard Medical School, Boston, MA, USA

Corresponding author: Dr. Christopher A. Walsh, Division of Genetics, Boston Children's Hospital, 300 Longwood Ave, CLS 15062.2, Boston, MA 02115, christopher.walsh@childrens.harvard.edu, Phone: 617-919-2923, Fax: 617-919-2010.
*These authors contributed equally to the work.

[5]Pediatric Neurology Unit, Department of Neurology, Massachusetts General Hospital, Boston, MA, USA

[6]Harvard-MIT Division of Health Sciences and Technology, Cambridge, MA, USA

[7]Department of Morphologic Sciences, Cayetano Heredia University, Lima, Perú

[8]Institute for Child Development, ARIE, Lima, Perú

[9]Stem Cell Program, Boston Children's Hospital, Boston, MA, USA

[10]Division of Hematology/Oncology, Boston Children's Hospital, Boston, MA, USA

[11]Dana-Farber Cancer Institute, Boston, MA, USA

[12]Department of Neurology, Boston Children's Hospital, Boston, MA, USA

[13]Complex Care Outpatient Program, Division of General Pediatrics, Boston Children's Hospital, Boston, MA, USA

[14]Department of Radiology and Biomedical Imaging, University of California, San Francisco, San Francisco, CA, USA

[15]Center for Integrative Brain Research, University of Washington, Seattle, WA, USA

[16]Department of Neurology, Harvard Medical School, Boston, MA, USA

Charged multivesicular body protein 1A/Chromatin modifying protein 1A (CHMP1A) is a member of the ESCRT-III (endosomal sorting complex required for transport-III) complex[1–2], but is also suggested to localize to the nuclear matrix and regulate chromatin structure[3]. Here we show that loss-of-function mutations to human *CHMP1A* cause reduced cerebellar size (pontocerebellar hypoplasia) and reduced cerebral cortical size (microcephaly). *CHMP1A* mutant cells show impaired proliferation, with increased expression of *INK4A*, a negative regulator of stem cell proliferation, and chromatin immunoprecipitation suggests a loss of the normal *INK4A* repression by BMI in these cells. Morpholino-based knockdown of zebrafish *chmp1a* resulted in brain defects resembling those seen after *bmi1a* and *bmi1b* knockdown, which were partially rescued by *INK4A* orthologue knockdown, further supporting links between CHMP1A and BMI1-mediated regulation of *INK4A*. Our results suggest that CHMP1A serves as a critical link between cytoplasmic signals and BMI1-mediated chromatin modifications that regulate proliferation of CNS progenitor cells.

As part of ongoing studies of human disorders of neural progenitor proliferation, we identified three families characterized by underdevelopment of the cerebellum, pons, and cerebral cortex (Fig. 1a–d). In a consanguineous pedigree of Peruvian origin, three children in two branches were affected (Fig. 1e; Family 1). Two additional pedigrees from Puerto Rico showed similar pontocerebellar hypoplasia and microcephaly (Fig. 1e; Family 2 and 3). Brain MRI of affected individuals from all families show severe reduction of the cerebellar vermis and hemispheres. Strikingly, the cerebellar folds ("folia") are relatively preserved despite the extremely small cerebellar size (Fig. 1a–d, Supplementary Videos 1, 2). All affected individuals had severe pontocerebellar hypoplasia, though affected individuals in

Family 1 showed better motor and cognitive function than those in Family 2 and 3 (Supplementary Note, Clinical Information).

Genome-wide linkage analysis of Family 1 and 2 using single nucleotide polymorphism (SNP) microarrays implicated only one region on chromosome 16q as linked and homozygous in all six affected individuals (Fig. 1e, Supplementary Fig. 1), with a maximum multipoint LOD score of 3.68 (Fig. 1e). Although Families 2 and 3 are not highly informative for linkage analysis, their shared homozygosity provides additional support for this locus. Furthermore, Families 2 and 3 shared the same haplotype (Supplementary Fig. 1), suggesting a founder effect. Sequencing of 42 genes within the candidate interval on 16q24.3 revealed homozygous variants predicted to be deleterious in the *CHMP1A* gene only. *CHMP1A* consists of seven exons encoding a 196 amino acid protein (Supplementary Note, *CHMP1A* isoforms). Affected individuals in Family 2 and 3 had a homozygous nonsense variant in exon 3, predicted to prematurely terminate translation (c.88C>T; Q30X; Fig. 2a). Family 1 showed a homozygous variant in intron 2 of *CHMP1A* (c.28-13G>A; Fig. 2a) predicted to create an aberrant splice acceptor site leading to an 11 base pair insertion into the spliced mRNA product (Supplementary Fig. 2a). The two mutations were absent from dbSNP, 281 neurologically normal European control DNA samples (562 chromosomes), the 1000 Genomes Project database[4], and approximately 5000 control exomes from the NHLBI Exome Sequencing Project. We sequenced *CHMP1A* in 64 individuals with other cerebellar anomalies without finding additional mutations, but none of these patients shared the rare and distinctive pattern of hypoplasia seen in the individuals with *CHMP1A* mutations.

RT-PCR analysis of *CHMP1A* in lymphoblastoid cells from affected individuals from Family 1 (CH3101 and CH3105) identified the predicted aberrant transcript with the 11 base pair insertion and a second aberrant transcript with a 21 base pair insertion, but no normal *CHMP1A* transcript (Supplementary Fig. 2b). In the parents of affected children from Family 1, and in unaffected control samples, only the normal transcript was detected, suggesting that the abnormal splice products are unstable. Western blot analysis revealed a single 24 kilodalton band in a normal control individual, but no corresponding band was detected in affected individuals from Families 1 or 2 (CH3101 and CH2401, respectively; Fig. 2c). Normalized to the loading control, levels of CHMP1A were 50% in the parent (CH3104). Hence this genetic study establishes *CHMP1A* null mutations as the cause of pontocerebellar hypoplasia and microcephaly in these pedigrees.

CHMP1A has been assigned two distinct putative functions, as both a <u>ch</u>romatin <u>m</u>odifying <u>p</u>rotein, and a <u>ch</u>arged <u>m</u>ultivesicular body <u>p</u>rotein[1,3]. CHMP1A was originally identified as a binding partner of the Polycomb group protein Pcl (Polycomblike)[3]. In the nucleus, it has been suggested to recruit the Polycomb group transcriptional repressor BMI1 to heterochromatin, and overexpressed CHMP1A has been shown to arrest cells in S-phase [3]. In the cytoplasm, CHMP1A is part of the ESCRT-III complex (endosomal sorting complex required for transport)[1–2]. ESCRT-III complex localizes to endosomes and interacts with VPS4A and VPS4B[5] to assist in the trafficking of ubiquitinated cargo proteins to the lysosome for degradation[6].

We investigated potential relationships of CHMP1A to Polycomb function by analysis of cell lines from two patients harboring different *CHMP1A* mutations (CH3101 from Family 1, and CH2401 from Family 2), which show severely impaired doubling times compared to control cell lines, suggesting essential roles of CHMP1A in regulating cell proliferation (Fig. 2d). In order to examine BMI1 function in these cells, we performed quantitative PCR analysis of expression of the BMI1 target locus *CDKN2A*, which encodes alternative transcripts *INK4A* (also known as $p16^{INK4a}$) and *ARF* (also known as $p14^{ARF}$) in human. This revealed abnormally increased expression of *INK4A*, the isoform implicated in cerebellar development, but not of *ARF* (Fig. 2e), suggesting de-repression of *INK4A*. Chromatin immunoprecipitation with a BMI1 antibody in control cell lines showed an approximately eight-fold enrichment of BMI1 binding at *INK4A* promoter DNA, relative to a control region 7kb upstream, whereas cells from an affected individual (CH2401) showed only about half this effect (Fig. 2f). Enrichment of BMI1 at the *ARF* promoter was not substantial in this assay, and was similar in both control and cell lines from affected individuals, consistent with the specificity of regulation of the *INK4A* isoform by BMI1 (Fig. 2f). Bmi1 suppresses the *Cdkn2a* locus via Polycomb-mediated H2A monoubiquitination, and is required for neural stem cell self-renewal[7]. Our evidence suggests a role for CHMP1A in mediating BMI1-directed epigenetic silencing at the *INK4A* promoter, but not at the *ARF* promoter.

We further explored the relationship between CHMP1A and BMI1 using morpholino-based knockdown experiments in zebrafish. Knockdown of the zebrafish *CHMP1A* orthologue (*chmp1a*) resulted in reduced cerebellum and forebrain volume, similar to the effects of human *CHMP1A* mutations and zebrafish knockdown of *BMI1* orthologues (Fig. 3a–e, Supplementary Fig. 3, 4). A second morpholino led to a similar phenotype, and both morpholinos were partially rescued by human *CHMP1A* mRNA, confirming the specificity (Supplementary Fig. 4). The cerebellum consists of 5 major cells types, with the principal cell, known as the Purkinje cell, deriving from the ventricular epithelium, whereas granule cells derive from a separate progenitor pool known as the rhombic lip. Granule cell precursors then migrate over the outer surface of the cerebellum and form the external germinal layer (EGL) before migrating radially past the Purkinje cells to settle in the internal granule layer (IGL)[8]. Within the *chmp1a* morphant cerebellum, the internal granule and molecular layers were severely affected (Fig. 3a, b), which is consistent with the relatively preserved folia pattern of the human cerebellum (thought to be primarily established by Purkinje cells) and severely reduced volume (determined mainly by granule cell quantity).

We then tested genetic interactions between *chmp1a* and the zebrafish orthologue of *INK4A* (*cdkn2a*). Knockdown of *cdkn2a* alone did not result in noticeable abnormalities, and double knockdown of *chmp1a* and *cdkn2a* resulted in partial rescue of the brain morphology defects seen with *chmp1a* knockdown (Fig. 3f, g). This was analogous to the rescue of the *Bmi1* knockout mouse cerebellar phenotype seen in the *Bmi1* and *Cdkn2a* double knockout mice[9]. Of note, there are also parallels in brain morphology between individuals with *CHMP1A* mutations and *Bmi1*-deficient mice, which show cerebellar hypoplasia[10–11] (Fig. 3h, i). In *Bmi1*-null mice, the cerebellar architecture was generally preserved, but the thickness of the granular and molecular layers was markedly reduced[10], and *Bmi1*-deficient mice show a

modest reduction in cerebral volume[10,12], similar to individuals with *CHMP1A* mutations (Supplementary Note, Clinical Information).

Subcellular localization of Chmp1a appears to vary depending on the cell type. Confocal images of NIH 3T3 cells show prominent exclusion of Chmp1a from the nucleus, where Bmi1 is seen (Fig. 4a). On the other hand, confocal images of HEK293T cells, while still showing predominantly cytoplasmic localization, show some nuclear immunoreactivity as well (Fig. 4b). Primary cultures of cerebellar granule cells also show predominant cytoplasmic localization, along with a speckled nuclear pattern (Fig. 4c). Overexpression of HA-tagged Chmp1a in cultured granule cells shows abundant nuclear Chmp1a with a punctate expression pattern, confirming the speckled nuclear localization of native Chmp1a (Fig. 4d), and consistent with earlier reports that Chmp1a can appear in the nucleus[3]. However, even with overexpression, Chmp1a and Bmi1 do not prominently co-localize within the nucleus, also in agreement with previous data[3].

Immunohistochemical studies of mouse developing cerebellum and cerebral cortex revealed widespread expression of Chmp1a in dividing and postmitotic cells. Chmp1a immunoreactivity is seen in the nucleus and cytoplasm of EGL, Purkinje and IGL cells (Fig. 4e, f, Supplementary Fig. 5). In the nucleus of these cells, Chmp1a immunoreactivity is seen in a speckled pattern. These speckles may be seen adjacent to Bmi1 signals, but they usually do not colocalize (Fig. 4f, Supplementary Fig. 5). At later stages of cerebellar development (P4, P10 and P29), Chmp1a expression persists in Purkinje and granule cells (Supplementary Fig. 6). E13.5 cerebral cortex shows widespread Chmp1a expression in the neuroepithelial cells (Fig. 4g). In the postnatal cerebral cortex (P4, P10 and P29), Chmp1a expression in postmitotic neurons of the cortical plate gradually decreases, and becomes almost undetectable by P29 (Supplementary Fig. 6). These expression studies confirm that Bmi1 and Chmp1a are often expressed in the same cells. On the other hand, the absence of widespread subcellular co-localization of Bmi1 and Chmp1a suggests that the regulation of Bmi1 by Chmp1a is perhaps not mediated by direct physical interaction.

Our data implicate CHMP1A as an essential CNS regulator of BMI1, which in turn is a key regulator of stem cell self-renewal. Chmp1a's dual cytoplasmic and nuclear localization, and its connection to the ESCRT-III complex, position Chmp1a as a potentially crucial link between cytoplasmic signals and the global regulation of stem cells via the Polycomb complex.

Online Methods

Genetic screening

The genetic study was approved by the Institutional Review Boards of Boston Children's Hospital and University of Chicago. Appropriate informed consent was obtained from all involved human subjects.

The affected individuals and their parents from Family 1 and the affected individuals from Family 2 were subjected to genome-wide SNP screen with Affymetrix GeneChip Human Mapping 250K Sty Array, performed at the Microarray Core of the Dana Farber Cancer

Institute. Microsatellite markers for fine mapping were identified using the UCSC Human Genome Browser[13] and were synthesized with fluorescent-labels (Sigma-Genosys). Two point and multipoint LOD scores were calculated using Allegro[14], assuming recessive inheritance with full penetrance and a disease allele frequency of 0.001. Sequencing primers were designed using Primer3[15], and genomic DNA was sequenced using standard Sanger technology. Control DNA samples from neurologically normal individuals of European descent were obtained from the Coriell Cell Repositories (Coriell Institute for Medical Research). All nucleotide numbers are in reference to *CHMP1A* isoform 2 cDNA (NM_002768, in which A of the ATG start site is +1) from the UCSC Genome Browser.

Analysis of *CHMP1A* splicing

Splice prediction software NetGene2[16] was used to determine the effect of the Family 1 allele on *CHMP1A* splicing. EBV-transformed lymphocytes were grown in RPMI-1640 with 15% (v/v) fetal bovine serum and 1% (v/v) penicillin/streptomycin in a humidified incubator at 37°C in 5% CO_2. RNA was isolated using the RNeasy Mini Kit (Qiagen). Total RNA (5μg) was used for first-strand synthesis with oligo(dT) primers and the SuperScript III First-Strand Synthesis SuperMix (Invitrogen), and 1μl of the product was used for the subsequent PCR reaction, with primers from 5′ UTR to exon 6 of *CHMP1A* (NM_002768). Primer sequences are listed in Supplementary Table 1.

Proliferation assay of lymphoblastoid cell lines

EBV-transformed lymphoblastoid cell lines from eight control subjects and two affected individuals (CH2401 and CH3101) were grown as described above. From each cell line, 20 million cells were grown, and then one million cells were aliquoted into four sets of five T25 flasks filled with 10ml of media. Each set was allowed to grow for 24, 48, 72, and 96 hours, respectively. Cell densities were estimated using a hemocytometer.

Quantitative PCR

EBV-transformed lymphoblastoid cell lines were grown and cDNA was generated as described above. *INK4A* and *ARF* levels were quantified using the StepOnePlus Real-Time PCR System (Applied Biosystems), with *GAPDH* as a control. Primer sequences are listed in Supplementary Table 1.

Chromatin immunoprecipitation

Chromatin immunoprecipitation (ChIP) was performed as previously described[17] with some modifications. For a single experiment, 20 million EBV-transformed lymphoblastoid cells and 4μg of the BMI1 antibody (Abcam, ab14389) were used. Quantitative PCR reactions were performed using SYBR Green reagents (Applied Biosystems) and StepOnePlus real-time PCR systems (Applied Biosystems). Primers were assessed for specificity by their melt curves, and a standard curve was determined using four ten-fold serial dilutions for each primer using the input DNA samples. Fold-enrichments for each ChIP sample were normalized to input Ct. Primer sequences are listed in Supplementary Table 1.

Zebrafish morpholino experiments

ATG-targeting morpholinos were designed against *chmp1a* (*chmp1a* MO #1), *bmi1a*, *bmi1b*, and the *INK4A* zebrafish orthologue (*cdkn2a*) (Gene Tools). In all experiments where *bmi1* morpholinos were used, *bmi1a* and *bmi1b* were injected together. Injections were performed at the one-cell stage. Optimal doses for the *chmp1a* MO #1*, bmi1a+b* and *ink4a* morpholinos were 4.5ng, 1.2ng, and 4.0ng, respectively. At 28 hours post-fertilization (hpf), the embryos were visualized using a stereo microscope (Zeiss). In order to confirm the specificity of the effects of the chmp1a MO #1 morpholino, a second ATG-targeting *chmp1a* morpholino (*chmp1a* MO #2) was designed. For this experiment, the dosage of *chmp1a* MO #1 and MO #2 injected was 6.0ng and 3.0ng, respectively. Morpholino sequences are listed in Supplementary Table 1.

For the rescue experiment, morphants were screened at 28hpf and scored for the presence of a defect in the angle of the head to the tail (measured at the otic vesicle) or a deviation in the straightness of the tail[18]. Human *CHMP1A* cDNA was PCR amplified from control human lymphoblastoid cell total RNA. Primer sequences are listed in Supplementary Table 1. The PCR product was subcloned into the pCS2+ vector, and 5′ capped mRNA was synthesized *in vitro* using the mMESSAGE kit (Ambion). mRNA was diluted in 0.1M KCl, and titrated for the rescue experiments.

For the histological preparation, morphants were grown at 28°C for 5 days, fixed overnight at 4°C in paraformaldehyde (PFA), then embedded in 3% low-melt agarose blocks (in phosphate buffered saline), which were fixed again in 4% PFA/PBS overnight. The fixed agarose blocks were embedded in paraffin and sectioned at 5μm thickness in the sagittal plane. Sections were stained by standard techniques with hematoxylin and eosin, and visualized using a brightfield microscope (Nikon).

For western blotting, zebrafish embryos were harvested at 48 hpf. They were dechorionated and deyolked as described[19], and treated with lysis buffer (10% SDS, 0.5M EDTA, 1X PBS) containing cOmplete Mini Protease Inhibitor Cocktail (Roche). Lysates were mixed with 2X Laemmli Sample Buffer, loaded onto NuPage 4–12% Bis-Tris gel (Invitrogen) and run at 100V for 2 hours. The gel was wet-transferred onto Immobilon-P transfer membrane (Millipore) at 300mA for 1.5 hours at 4 C. The membrane was blocked with Odyssey Blocking Buffer (LI-COR), and incubated with antibodies against Chmp1a (1:100; Abcam, ab104103) and beta-actin (1:10000; Abcam, ab6275), and then with IRDye secondary antibodies (LI-COR, 926–32212 and 926–68023). LI-COR Imaging System was used for imaging and quantification.

Immunocytochemistry and immunohistochemistry

NIH 3T3 and HEK293T cells were grown in DMEM with 10% (v/v) fetal bovine serum and 1% (v/v) penicillin/streptomycin, fixed and stained with antibodies against Chmp1a (1:200; Abcam, ab36679) and Bmi1 (1:250; Abcam, ab14389) using standard techniques, and visualized on a confocal microscope (Nikon).

All animal work was approved by Harvard Medical School, Beth Israel Deaconess Medical School and Boston Children's Hospital Institutional Animal Care and Use Committees.

Cerebellar granule neuron cultures from euthanized, postnatal day 5 mouse pups were prepared as described[20]. After dissociation, cell density was measured using a hemocytometer and one million cells were plated on each poly-L-ornithine-coated coverslip with 500μL plating media in a 24-well plate. After one day in vitro (DIV) in a 37 C incubator, 20μL of 250μM AraC (cytosine-1-β-D-arabinofuranoside) was added to each well to arrest mitosis of non-neurons. At 2 DIV, the conditioned media was collected from each well, and the wells were washed with DMEM. The cells were then transfected with the HA-Chmp1a mammalian expression construct (GeneCopoeia, EX-Mm15805-M06). Transfection solution (87.6uL HBSS, 4.4μL of 2.5M calcium chloride, with 1.5μg of plasmid DNA) was prepared at room temperature, and 35μL of the transfection solution was added to a total of 400μL of conditioned media to each well. After 36 additional hours (4 DIV), cells were fixed with 4% PFA for 20 minutes at room temperature, washed with PBS, and stained with antibodies against HA (1:100; Abcam, ab9110) and Bmi1 (1:250; Abcam, ab14389). Untransfected cells were processed similarly and stained with antibodies against Chmp1a (1:200; Abcam, ab36679) and Bmi1.

Tissues were perfused with 4% PFA, dissected and fixed overnight in 4% PFA, then embedded in paraffin and sectioned at 5 or 8μm. After rehydration of the slides in serial washes with xylene, 50% xylene/ethanol, 100%/70%/50%/30% ethanol, and finally PBS, the slides were boiled in antigen retrieval solution (Retrievagen A; BD Biosciences) for 8 minutes in the autoclave. Slides were blocked with PBS with 0.1% Triton-X100 supplemented with 1% donkey serum for 1 hour at room temperature, followed by addition of antibodies against Bmi1 (1:400; Millipore, clone F6), Chmp1a (1:300; Abcam, ab36679 and ab104103) or calbindin (Swant, CB300) in the blocking solution for overnight incubation at 4 C. Slides were washed 3×5 minutes in PBS, and then developed with secondary antibodies conjugated to Alexa-Fluor dyes (Invitrogen) for 1.5 hours at room temperature. Slides were again washed 3×5 minutes in PBS, then mounted with Fluoromount-G (SouthernBiotech) containing DAPI (1:1000), and visualized on a confocal microscope (Nikon) or fluorescence microscope (Zeiss). For E13.5 and P2 cerebral cortex, frozen section specimens were used. For frozen sections, heads of E13.5 mouse embryos were directly fixed in 4% PFA, and P2 pups were perfused with 2ml 1X PBS and then with 4ml 4% PFA in PBS, followed by overnight fixation in 4% PFA. They were then placed in gradually increasing sucrose solutions (10%/15%/30%), each overnight, for cryopreservation, followed by embedding in OCT and sectioning at 20μm thickness. The same antigen retrieval and staining procedure as the paraffin-embedded sections was used.

Supplementary Material

Refer to Web version on PubMed Central for supplementary material.

Acknowledgments

References

1. Howard TL, Stauffer DR, Degnin CR, Hollenberg SM. CHMP1 functions as a member of a newly defined family of vesicle trafficking proteins. J Cell Sci. 2001; 114:2395–404. [PubMed: 11559748]

2. Tsang HT, et al. A systematic analysis of human CHMP protein interactions: additional MIT domain-containing proteins bind to multiple components of the human ESCRT III complex. Genomics. 2006; 88:333–46. [PubMed: 16730941]

3. Stauffer DR, Howard TL, Nyun T, Hollenberg SM. CHMP1 is a novel nuclear matrix protein affecting chromatin structure and cell-cycle progression. J Cell Sci. 2001; 114:2383–93. [PubMed: 11559747]

4. Consortium GP. A map of human genome variation from population-scale sequencing. Nature. 2010; 467:1061–73. [PubMed: 20981092]

5. Stuchell-Brereton MD, et al. ESCRT-III recognition by VPS4 ATPases. Nature. 2007; 449:740–4. [PubMed: 17928862]

6. Scita G, Di Fiore PP. The endocytic matrix. Nature. 2010; 463:464–73. [PubMed: 20110990]

7. Molofsky AV, et al. Bmi-1 dependence distinguishes neural stem cell self-renewal from progenitor proliferation. Nature. 2003; 425:962–7. [PubMed: 14574365]

8. Garel C, Fallet-Bianco C, Guibaud L. The fetal cerebellum: development and common malformations. J Child Neurol. 2011; 26:1483–92. [PubMed: 21954430]

9. Jacobs JJ, Kieboom K, Marino S, DePinho RA, van Lohuizen M. The oncogene and Polycomb-group gene bmi-1 regulates cell proliferation and senescence through the ink4a locus. Nature. 1999; 397:164–8. [PubMed: 9923679]

10. Leung C, et al. Bmi1 is essential for cerebellar development and is overexpressed in human medulloblastomas. Nature. 2004; 428:337–41. [PubMed: 15029199]

11. van der Lugt NM, et al. Posterior transformation, neurological abnormalities, and severe hematopoietic defects in mice with a targeted deletion of the bmi-1 proto-oncogene. Genes Dev. 1994; 8:757–69. [PubMed: 7926765]

12. Zencak D, et al. Bmi1 loss produces an increase in astroglial cells and a decrease in neural stem cell population and proliferation. J Neurosci. 2005; 25:5774–83. [PubMed: 15958744]

13. Kent WJ, et al. The human genome browser at UCSC. Genome Res. 2002; 12:996–1006. [PubMed: 12045153]

14. Gudbjartsson DF, Jonasson K, Frigge ML, Kong A. Allegro, a new computer program for multipoint linkage analysis. Nat Genet. 2000; 25:12–3. [PubMed: 10802644]

15. Rozen, S.; Skaletsky, HJ. Primer3 on the WWW for general users and for biologist programmers. In: Krawetz, S.; Misener, S., editors. Bioinformatics Methods and Protocols: Methods in Molecular Biology. Humana Press; Totowa, New Jersey: 2000. p. 365-386.

16. Brunak S, Engelbrecht J, Knudsen S. Prediction of human mRNA donor and acceptor sites from the DNA sequence. J Mol Biol. 1991; 220:49–65. [PubMed: 2067018]

17. Flavell SW, et al. Genome-wide analysis of MEF2 transcriptional program reveals synaptic target genes and neuronal activity-dependent polyadenylation site selection. Neuron. 2008; 60:1022–38. [PubMed: 19109909]

18. Kimmel CB, Ballard WW, Kimmel SR, Ullmann B, Schilling TF. Stages of embryonic development of the zebrafish. Dev Dyn. 1995; 203:253–310. [PubMed: 8589427]

19. Link V, Shevchenko A, Heisenberg CP. Proteomics of early zebrafish embryos. BMC Dev Biol. 2006; 6:1. [PubMed: 16412219]

20. Bilimoria PM, Bonni A. Cultures of cerebellar granule neurons. CSH Protoc. 2008 2008, pdb prot5107.
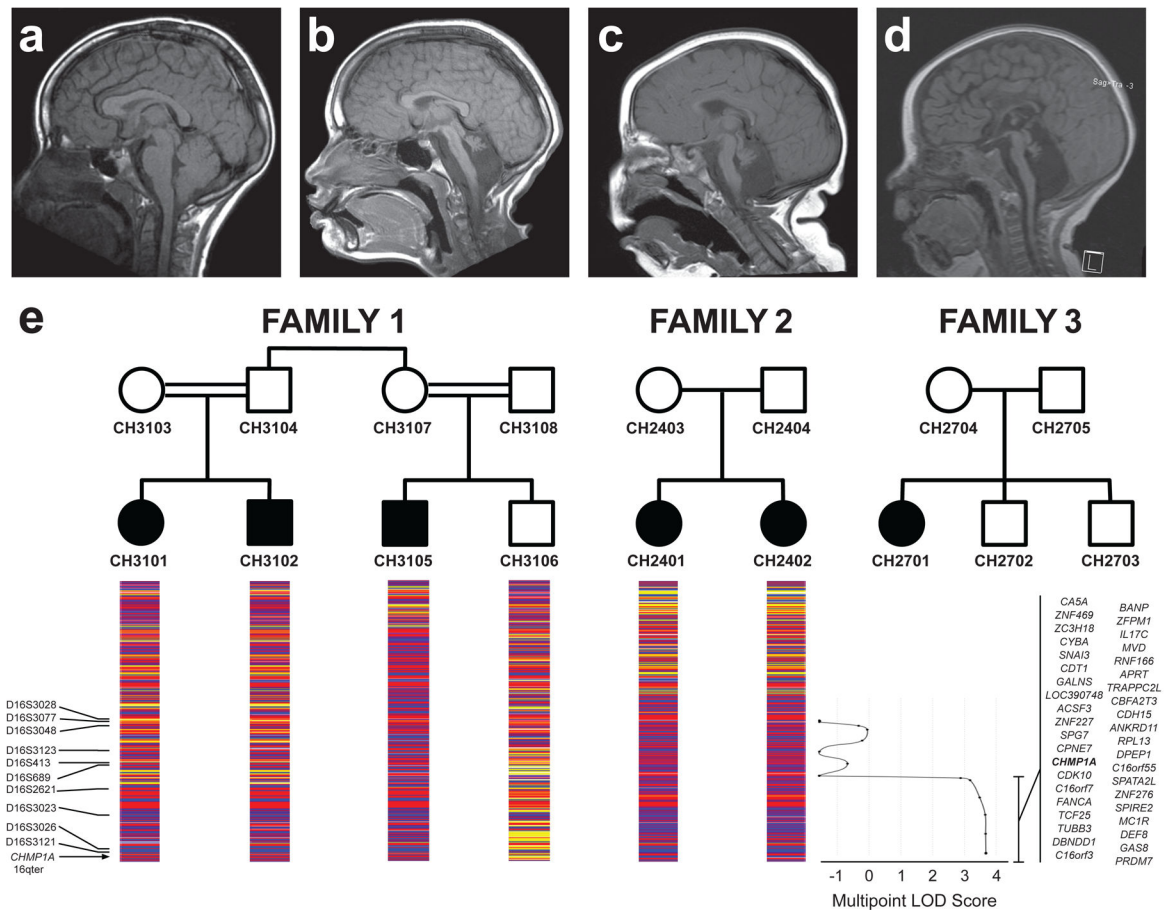
Figure 1. Brain MRI and linkage mapping of pontocerebellar hypoplasia with microcephaly
(a–d) T1-weighted sagittal brain MRI images of a neurologically normal individual (a) and
affected individuals CH3102 (b), CH2402 (c), and CH2701 (d) are shown. Compared to
control, affected individuals show mild reduction in cortical volume, thinning of the corpus
callosum, and severe hypoplasia of the pons, cerebellar vermis, and cerebellar hemispheres.
(e) Family 1 is a consanguineous pedigree from Peru in which three children from two
branches are affected. Family 2 and 3 are both from Puerto Rico. Below each child in
Family 1 and 2 is their Affymetrix 250K Sty SNP data (red and blue = homozygous SNP
call; yellow = heterozygous SNP call), showing a region of homozygosity shared by all
affected individuals in distal chromosome 16q. The graph aligned with the SNP genotyping
data shows multipoint LOD scores calculated from microsatellite maker analysis of Family
1. Genes in the region of LOD > 3 are indicated to the right of the graph.
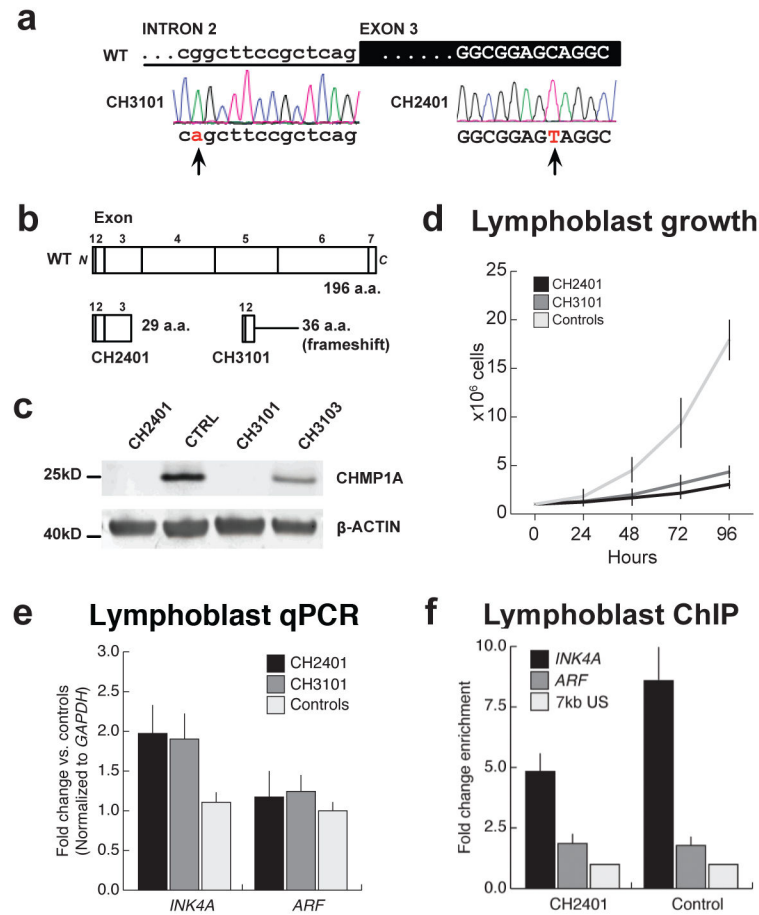
Figure 2. Loss-of-function mutations in *CHMP1A*, and dysregulation of *INK4A* in cell lines from affected individuals

(a) Chromatograms of genomic DNA sequencing show homozygous mutations in intron 2 (CH3101; c.28-13G>A) and in exon 3 (CH2401; c.88C>T). Mutations are highlighted in red with arrows. (b) A schematic diagram of full length CHMP1A showing the relative contribution of each exon to the 196 amino acids of the protein. The expected effect of the mutation in CH2401 is a premature termination of translation after 29 amino acids. The intronic mutation in CH3101 creates a novel splice acceptor site, and usage of this novel acceptor causes a frameshift after exon 2, resulting in a termination of translation after 36 amino acids. (c) Western blot analysis of lysates from lymphoblastoid cell lines from CH2401 and CH3101 demonstrates a complete loss of expression of a 24 kD band detected by a CHMP1A antibody in control lysate (CTRL). Lysates from a cell line generated from CH3103 (the mother of CH3101) shows 50% of protein level relative to control. Levels of protein expression were normalized to the 40 kD beta-actin loading control band. (d) Lymphoblastoid cell lines from CH2401 and CH3101 proliferate at a much lower rate compared to control cell lines, tracked over a 4 day period. (e) Quantitative PCR (qPCR) of cDNA levels from human lymphoblastoid cell lines from CH2401 and CH3101 show a nearly two-fold increase in expression of *INK4A* relative to an unrelated, neurologically normal control cell line (normalized to *GAPDH* expression levels). The other transcribed isoform at the locus, *ARF*, shows no significant difference in expression level between cells

from affected individuals and control. (f) Chromatin immunoprecipitation (ChIP)-qPCR from lymphoblastoid cell lines using a BMI1 antibody shows an approximate eight-fold enrichment of *INK4A* promoter DNA relative to probes targeted 7kb upstream (7kb US) of the locus in a control cell line. This enrichment is reduced by nearly half in cell lines derived from CH2401 with a homozygous mutation in *CHMP1A*. However, enrichment at the *ARF* promoter is not significantly different from the control cell line. Error bars in the graphs (d-f) represent standard error of the mean.
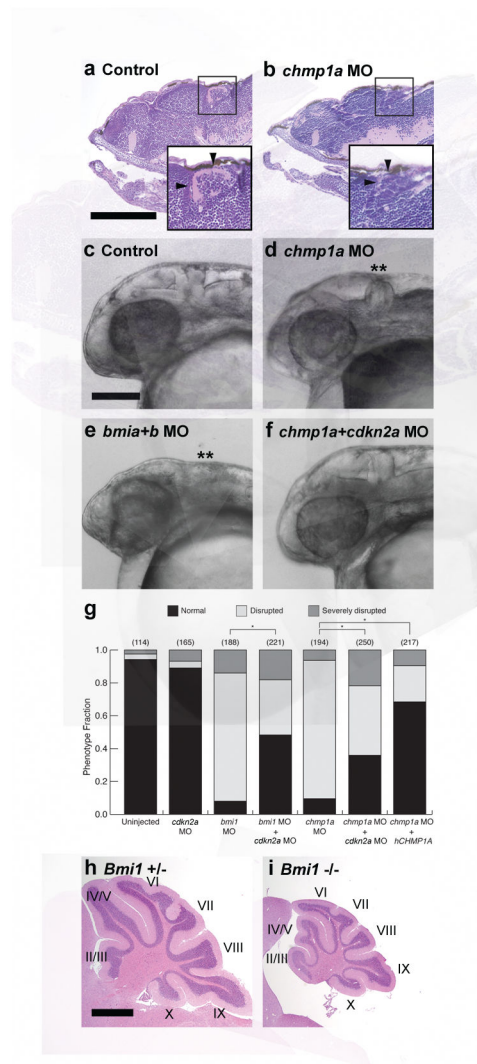
Figure 3. Genetic links between *CHMP1A* and *BMI1* in zebrafish and mice
(a, b) Compared to parasagittal section of control zebrafish 5 days post fertilization (a), zebrafish injected with *chmp1a* morpholino (MO) show a reduction in cerebellum and forebrain volume. Higher magnification images of the cerebellum (insets) highlight loss of molecular and internal granular layers in the mutant (arrowheads). (c-g) Compared to control zebrafish (c), morpholino-based knockdown of *chmp1a* (d) shows a reduction in head size, with the hindbrain more markedly reduced in thickness (asterisks), which is similar to the phenotype seen by knocking down the zebrafish orthologues of BMI1, *bmi1a* and *bmi1b* (e). When the *cdkn2a* morpholino is co-injected with the *chmp1a* morpholino, the *chmp1a* knockdown phenotype is partially rescued (f). Embryos are classified at 28 hours post fertilization as either normal, disrupted, or severely disrupted (see Online Methods) for each of uninjected controls, *cdkn2a* MO, *bmi1* MO *chmp1a* MO, *bmi1* MO coinjected with *cdkn2a* MO, and *chmp1a* MO coinjected with *cdkn2a* MO or human *CHMP1A* mRNA (g). (h, i) Compared to the wildtype mouse cerebellum at P25 (h), sagittal cross-sectional area of the *Bmi1*−/− mouse cerebellum at the same age (i) is dramatically reduced, though foliation
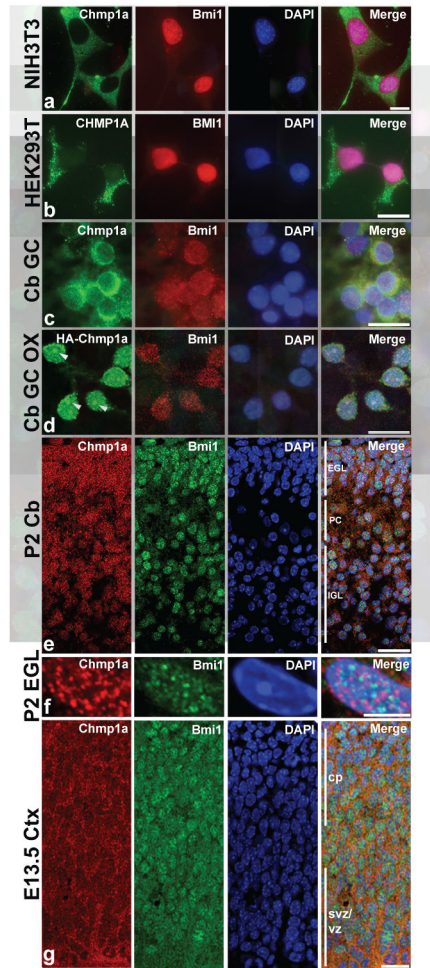
and structure of the lobules (indicated in Roman numerals) are generally preserved. Scale bars = 200μm (a, b), 200μm (c–f), 500μm (h, i). Asterisk = $p < 0.001$, two-tailed Pearson's chi-squared test (g).

Figure 4. Chmp1a and Bmi1 expression in cultured cells and the developing mouse brain
(a) Immunocytochemistry of NIH 3T3 cells shows cytoplasmic Chmp1a staining with exclusion from the nucleus, where Bmi1 is present. (b) Immunocytochemistry of HEK293T cells also shows cytoplasmic Chmp1a staining, with some nuclear immunoreactivity. (c) In dissociated cerebellar granule cells (Cb GC), endogenous Chmp1a localizes mostly to the cytoplasm, but also has a speckled nuclear localization. (d) When dissociated cerebellar granule cells are transfected with an HA-tagged Chmp1a overexpression construct (Cb GC OX), HA-Chmp1a is expressed robustly in the nucleus with prominent nuclear puncta (arrowheads). (e) In the developing cerebellum at postnatal day 2 (P2 Cb), Chmp1a is expressed in the nucleus and cytoplasm of cells in the external germinal layer (EGL), Purkinje cells (PC) and cells in the internal granule layer (IGL). Bmi1 is expressed in these cells that are positive for Chmp1a, and it primarily localizes to the nucleus. (f) In the nucleus of P2 EGL cells (P2 EGL), Chmp1a shows speckled staining. The Chmp1a signals are sometimes seen adjacent to the Bmi1 signals, but they rarely colocalize. (g) In the developing cerebral cortex at E13.5 (E13.5 Ctx), Chmp1a is expressed in both ventricular zone progenitors and cortical plate cells. Bmi1 is expressed in the same population of cells.

svz/vz = subventricular and ventricular zones. cp=cortical plate. Scale bars = 20μm (a–e, g), 5μm (f).